LOMONOSOV MOSCOW STATE UNIVERSITY

SKOBELTSYN INSTITUTE OF NUCLEAR PHYSICS (SINP)

A.N. Ermakov, V.A. Khankin, Yu.A. Kubyshin, N.I Pakhomov, J.P. Rigla, V.I. Shvedunov

DESIGN AND MAGNETIC MEASUREMENTS OF THE EXTRACTION MAGNET FOR 55 MeV RACE TRACK MICROTRON

MSU-SINP Preprint No 2011-2/866

UDC 621.039

A.N. Ermakov, V.A. Khankin, Yu.A. Kubyshin, N.I Pakhomov, J.P. Rigla, V.I. Shvedunov

E-mail addresses: shved@depni.sinp.msu.ru

DESIGN AND MAGNETIC MEASUREMENTS OF THE EXTRACTION MAGNET FOR 55 MeV RACE TRACK MICROTRON

Preprint MSU-SINP N 2011-2/866

Abstract

We describe results of optimization of the extraction magnet of a 55 MeV Race-Track Microtron (RTM). Because of small spacing between the RTM orbits special attention has been paid to optimization of magnetic screens with the aim to decrease the influence of stray magnetic fields on the accelerated beam. Results of simulations with 2D and 3D codes are compared with magnetic field distribution measurements.

А.Н. Ермаков, В.А. Ханкин, Ю.А. Кубышин, Н.И. Пахомов, Х.П. Ригла, В.И. Шведунов

РАЗРАБОТКА И МАГНИТНЫЕ ИЗМЕРЕНИЯ МАГНИТА ВЫВОДА 55 МэВ РАЗРЕЗНОГО МИКРОТРОНА

Препринт НИИЯФ МГУ № 2011 – 2/866

Аннотация

Описаны результаты оптимизации магнита вывода 55 МэВ разрезного микротрона. Из-за близкого расположения орбит разрезного микротрона специальное внимание было уделено оптимизации магнитных экранов с целью уменьшения влияние рассеянных магнитных полей на ускоряемый пучок. Результаты компьютерного моделирования с использованием 2D и 3D программ сравниваются с измерениями распределения магнитного поля.

INDEX

1. – Introduction.

Skobletsyn Institute of Nuclear Physics of the Moscow State University and P.N. Lebedev Physics Institute are currently carrying out the commissioning of a 55 MeV Race - Track Microtron dedicated to the detection of explosives using the photonuclear technique [1,2]. The main parameters of the RTM reached at the commissioning are given in Table 1 and an RTM general view is presented in Fig.1.

Table 1: RTM parameters.

Output energy	55 MeV
Output pulse current	10 mA
Repetition rate	5 – 50 Hz
Number of linac passages	11
Energy gain/turn	5 MeV
Current pulse length	5 μs
Operating frequency	2856 MHz
End magnet field	1.0 T
Maximum RF power	2.5 MW

Figure 1: 55 MeV RTM general view

In this paper we describe the design, construction and measurements of the extraction magnet of this RTM. The paper is organized as follows. In Sect. 2 main characteristics of the magnet and its initial 2D design obtained by using the PANDIRA code are described. In Sect. 3 a magnet design with a system of passive frontal screens whose function is to reduce stray fields is discussed. In Sect. 4 an optimization of the screen system obtained by using the ANSYS code [3] is described. Results of the experimental measurements carried out in order to verify the new screen design are reported in Sect. 5.

2. – Extraction magnet description.

The extraction magnet deflects the accelerated 55.5 MeV electron beam from the last RTM orbit and directs it to an experimental area. The extraction magnet position inside the RTM is shown schematically in Fig. 2.

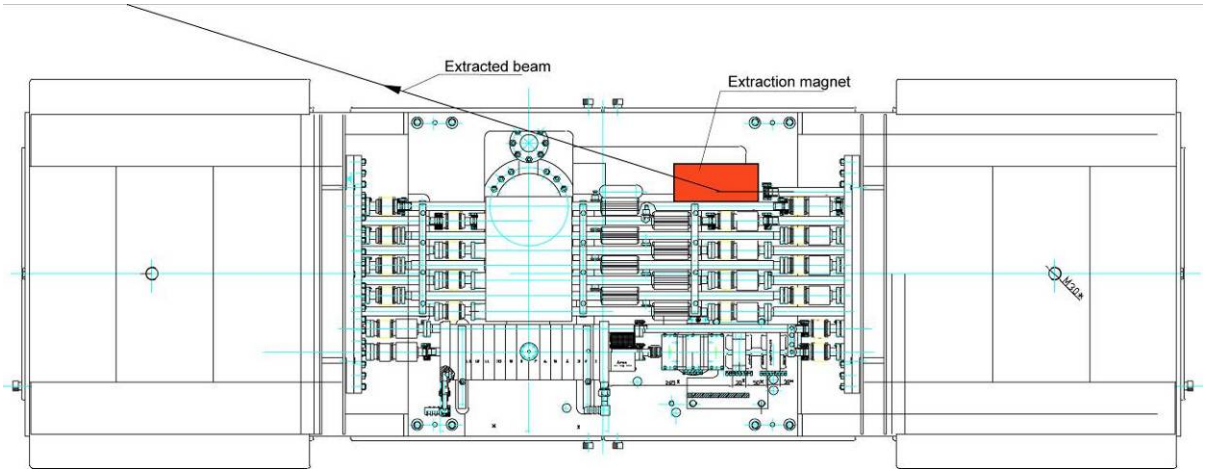

Figure 2: RTM with the extraction magnet shown.

In order to avoid the extracted beam intersection with RTM elements the extraction angle of 17.5º and extraction magnet effective length equal to 175 mm were chosen. The magnetic field induction necessary to provide such angle for 55 MeV electrons is 0.3181 T.

To describe the beam trajectory and location of extraction magnet elements we introduce a coordinate system shown in Fig. 3. It was also used in ANSYS simulations and magnetic field measurements described below. As one can see, the positions of the beam at the entrance and exit of the extraction magnet with respect to the z-axis are x= -13.5 mm and x=13.5 mm, respectively.

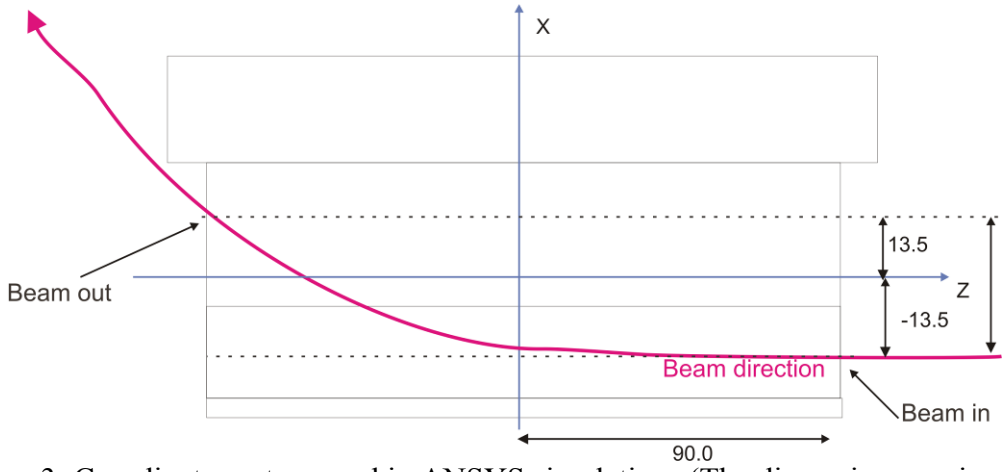

Figure 3: Coordinate system used in ANSYS simulations (The dimensions are in mm).

Different versions for the extraction magnet design have been studied. Initially a frame type design of an electromagnet with excitation coils was considered, its cross section is shown in Fig.4. There the beam positions at the entrance and exit of the extraction magnet are also indicated. The width of the region spanned by the beam is 27 mm and the distance between the 55.5 and 50.5 MeV orbits is 33.0 mm. However this

design has a problem of excessive coil current, namely with the diameter of machined cooling water channels , the current density in the coil would be well above 30 A/mm^2 and with a few turns of the coil the power supply current would be as high as ~1000 A.

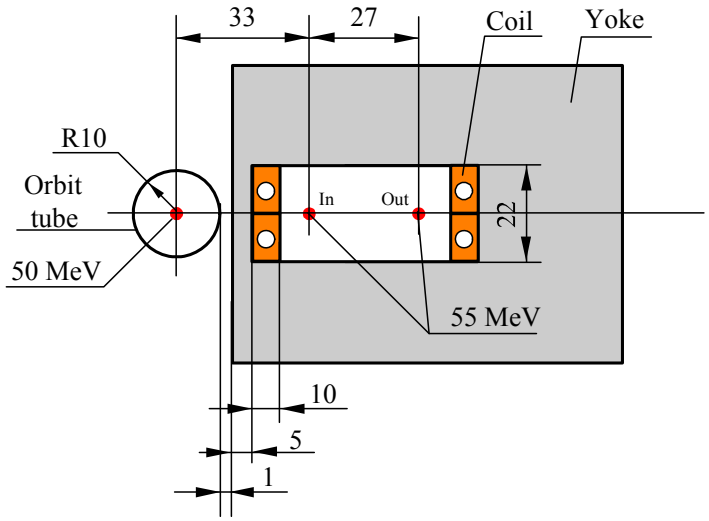

Figure 4: Cross section of the window frame extraction magnet. Dimensions are given in mm.

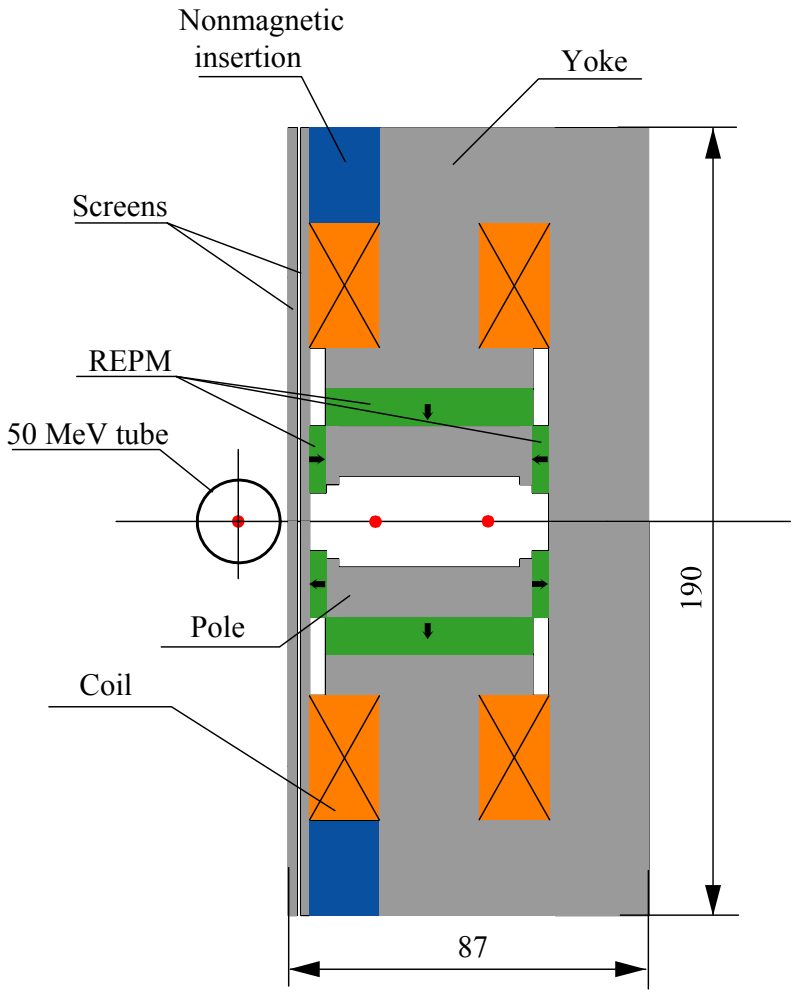

Figure 5: Cross section of the hybrid extraction magnet. Dimensions are in mm.

Different possibilities to reduce the coil current were analyzed, in particular (1) decrease of the bending angle, (2) increase of the magnet length, (3) use of a pulsed magnet. However, in the first case it would be necessary to drill a hole in the end magnet yoke for beam passage, in the second to increase the distance between the end magnets thus increasing the RTM dimensions, and in the third to build a pulsed magnet with a 3000 A current and 30 μs pulses following with the frequency 50 Hz.

These three possibilities were rejected as non-optimal and it was decided to use a hybrid magnet in which the required magnetic field level is produced by a rare earth permanent magnetic material (REPM) and excitation coils are used only to adjust the field level. The initial design of the extraction magnet was performed with the 2D code PANDIRA. The cross section of this hybrid extraction magnet is given in Fig.5.

The magnet consists of a yoke, poles, REPM (Nd-Fe-B) blocks, excitation coils, *two lateral magnetic screens* with an air gap between them and non-magnetic insertions. The residual magnetization of the REPM material necessary to produce the required magnetic field in the 22.0 mm height gap is 0.8924 T. The maximum current in the coils is 2A, the number of turns is 250, the coil area is 510 mm^2 and the filling factor is equal to 0.8. The maximum current density in the wire of the diameter 1.0 mm is 2.5 A/mm^2. For this design the cooling of the coils is not necessary.

The shape of the poles and lateral REPM blocks were optimized with the aim to obtain a field uniformity in the region of the beam passage about 1%. In Fig.6 the median plane field distributions for the total coil currents $I_{total} = \pm 500\text{ATurns}$ and $I_{total} = 0\text{ATurns}$ are shown. The field level can be varied within the ±5 % interval that corresponds to the ±2.75 MeV variation of the last orbit energy.

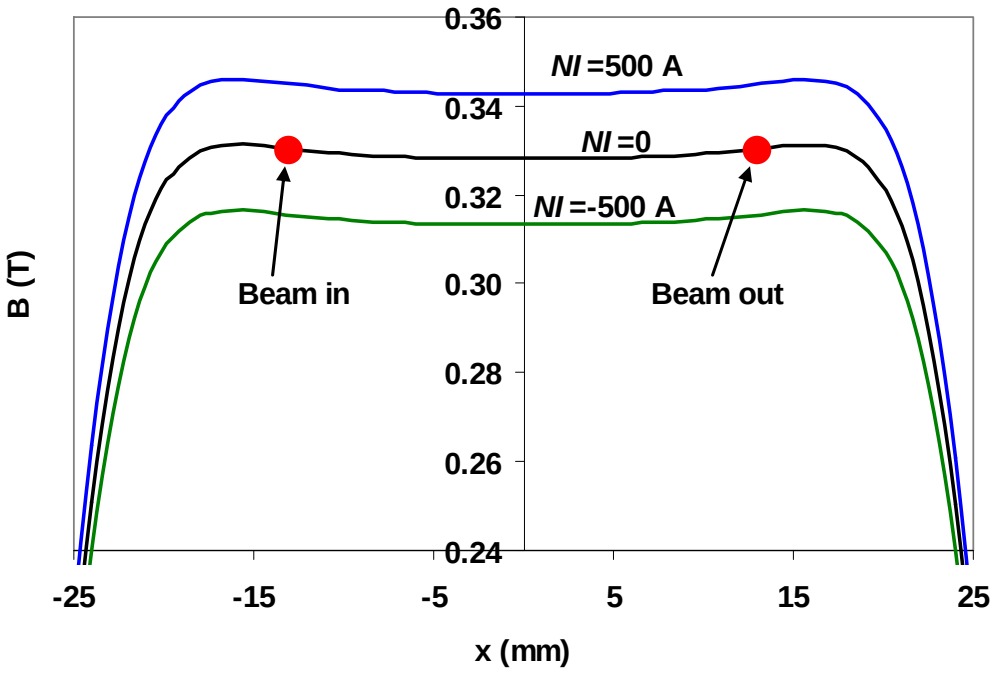

Figure 6: Median plane field distributions for different values of the total coil current.

3. – Original magnet design.

The original design of the extraction magnet did not include magnetic screens at the entrance and exit. Due to the fringe field its measured effective length appeared to be 192 mm as compared to 175 mm used in preliminary field estimations. In order to provide the 17.5^0 beam deflection angle of the 55.5 MeV orbit the field level was tuned to the value 0.285 T .

During the RTM commissioning it was found that stray magnetic fields from the extraction magnet in the region of the 9-th and 8-th (50.5 MeV and 45.5 MeV) orbits were producing a considerable deflection of the beam that could not be compensated by steering coils installed at RTM orbits.

To solve this stray field problem additional *passive frontal screens* of the 2.0 mm thickness have been placed at the entrance and exit of the extraction magnet. The material used for these screens was steel 1010. In Fig.7 two images of the magnet with these upstream and downstream screens are given. Due to the screens the effective length of the magnet has decreased to 180 mm and the maximum coil current appeared to be insufficient. In order to provide the required magnetic field level equal to 0.325 T the REPM residual magnetization was increased.

The installation of the screens did not solve the stray field problem completely. Therefore, in order to reduce the stray field effect on the 50.5 MeV orbit an additional μ – metal magnetic cylindrical cover around the 9-th orbit vacuum tube was installed. This cover is shown in Fig.8. However, it does not give solution of the stay field problem either.

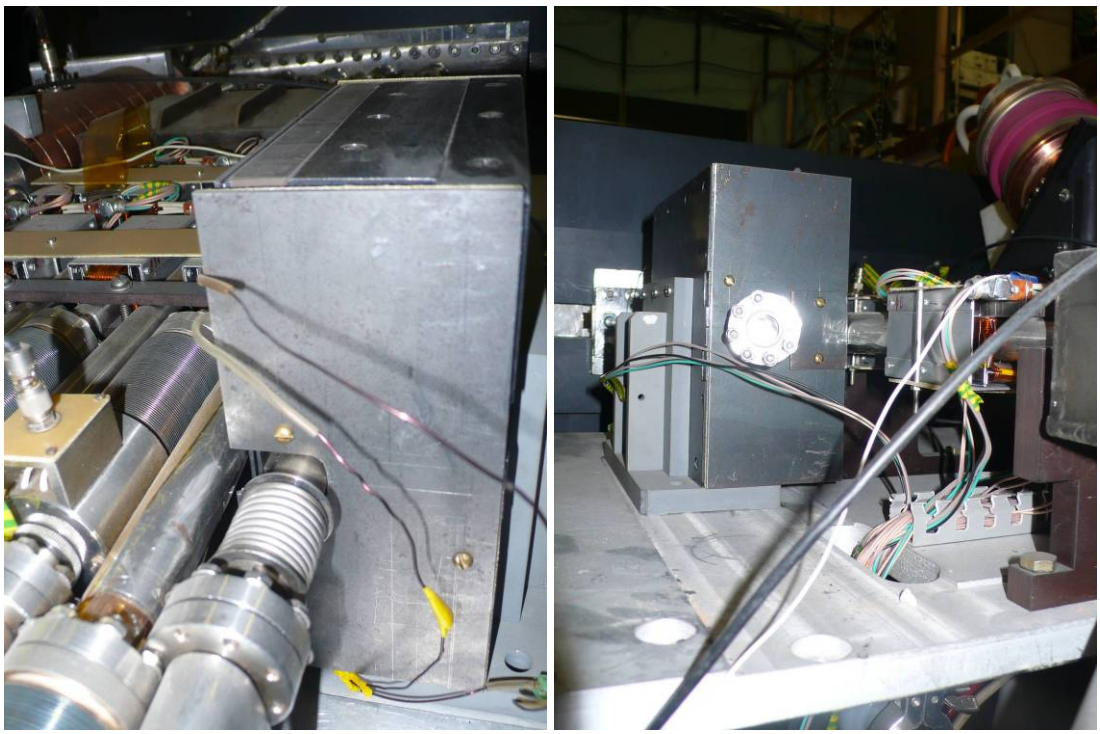

(a) (b)

Figure 7: The extraction magnet with the upstream (a) and downstream (b) screens.

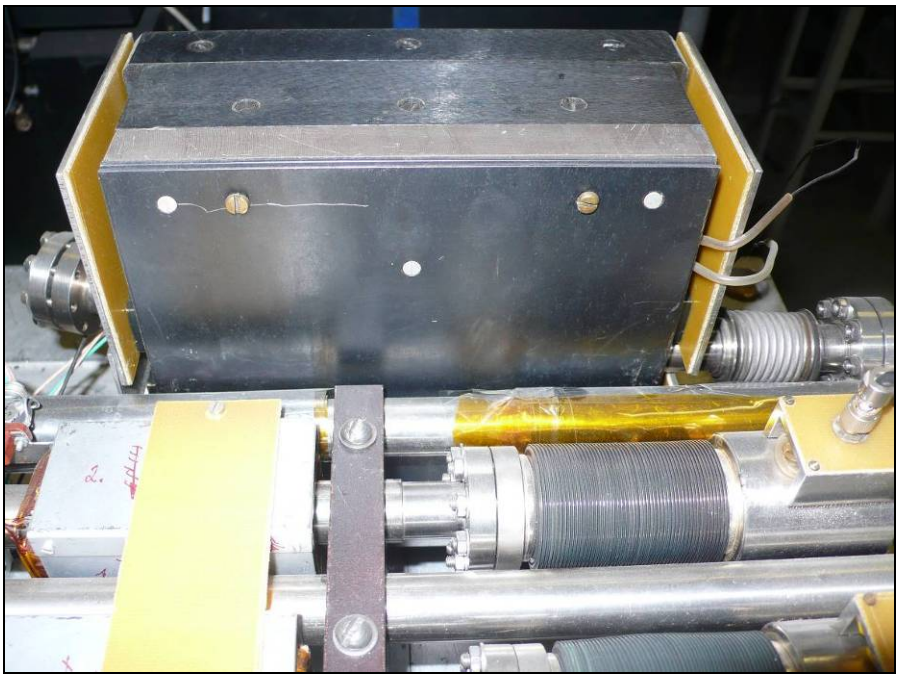

Figure 8: The cylindrical cover for the shielding of the 50.5 MeV orbit.

4. - Magnetic screen system optimization

To reduce the stray fields to an acceptable level a more detailed 3D study of the magnetic field distribution and subsequent 3D optimization of the screen geometry is needed. These improvements were carried out using the ANSYS code. An ANSYS model without screens used in the numerical calculations is shown in Fig. 9. In fact, taking into account the magnet symmetry, the simulations were done for a 1/4 of the magnet geometry the appropriate boundary conditions imposed.

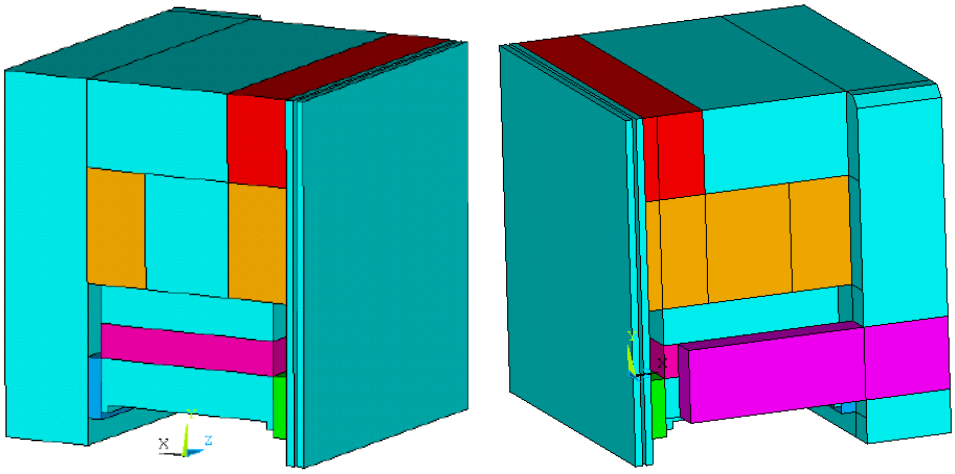

(a) (b)

Figure 9: ANSYS geometry: symmetry plane (a) and entrance plane (b) views.

The procedure of optimization of the screen system was carried out with the condition that the deflection angle caused by the stray magnetic field at the 9-th orbit must be less than 0.15 mrad, a value which can be easily compensated by the steering coils at the orbits. In order to obtain the required magnetic field of 0.325 T in a 22.0 mm height gap and for the magnetic permeability of the REPM material equal to 1.03 the residual magnetization was set to be 0.978 T.

We followed the following optimization process:

Step 1: The upstream and downstream screens with the rectangular beam aperture were replaced by screens with a circular aperture of radius 12.0 mm. In Fig.10 a 3D extraction magnet design with the rectangular and circular beam apertures is shown. The magnetic field distribution in the orbit plane at the upstream screen position is given in Fig. 11. In this case the magnetic field integral is equal to 1.9158×10^{-4} T·m which corresponds to a deviation of the 50.5 MeV orbit with the bending angle 1.2 mrad. This value is lower than the one obtained in the original model, although it is still higher than the allowed upper limit for the bending angle.

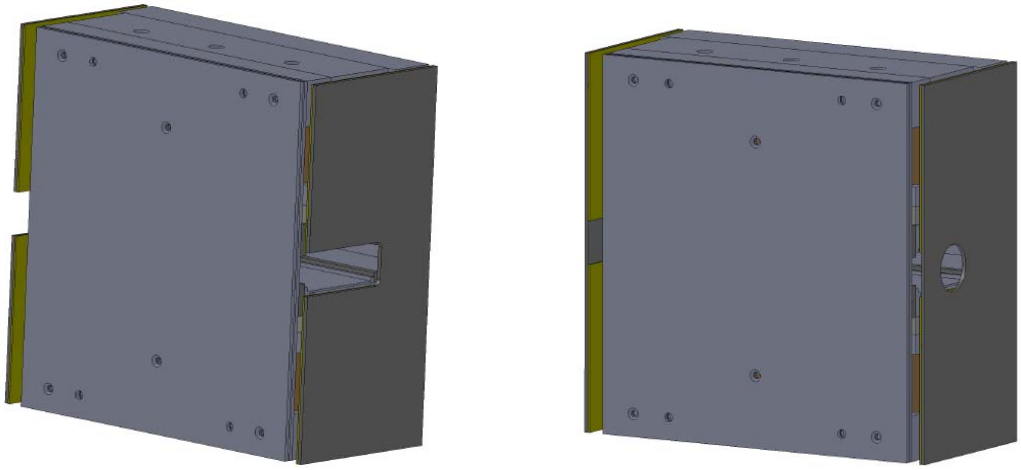

(a) (b)

Figure 10: 3D extraction magnet design with rectangular (a) and circular (b) screen apertures.

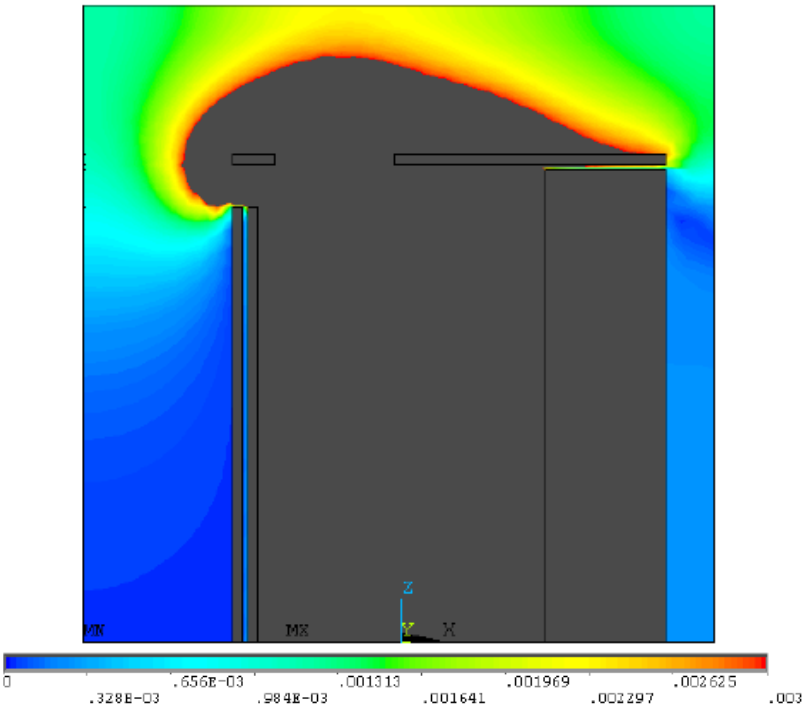

Figure 11: Magnetic flux density distribution, B_{sum}, in the orbit plane for the range $0.0 < B_{sum} < 0.003$ T after step 1.

Step 2: The length of the *outer lateral screen* was increased by 7.5 mm at each side so that the gap between the lateral and frontal screens is eliminated. The thickness of this screen is limited by the distance between the extraction magnet and vacuum tube of the 9th orbit. In Fig.12 the 3Dextraction magnet design with initial (a) and modified (b) lateral screens is shown. The magnetic field distribution in the orbit plane is shown in Fig. 13. Comparing it to the one in Fig. 11 one can see that the increase of the length of the lateral screen has reduced the level of the stray field considerably. In this case the value of the *y*-component of the magnetic field integral is equal to 5.922×10^{-5} T·m, the corresponding angle of deviation of the 50.5 Mev orbit is 0.3612 mrad. Again, this value is lower than the one obtained in the original model, but still exceeds the upper limit for the bending angle.

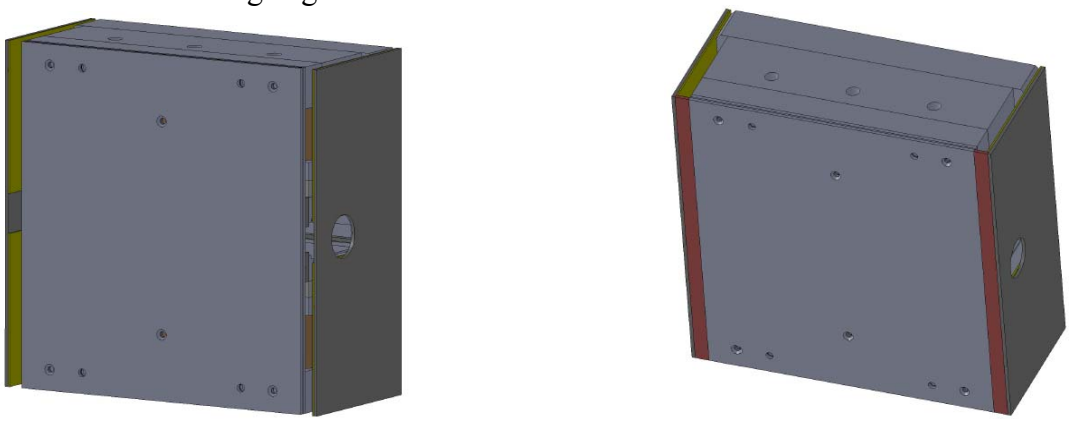

(a) (b)

Figure 12: 3D extraction magnet design with the initial (a) and modified (b, red parts) lateral screens.

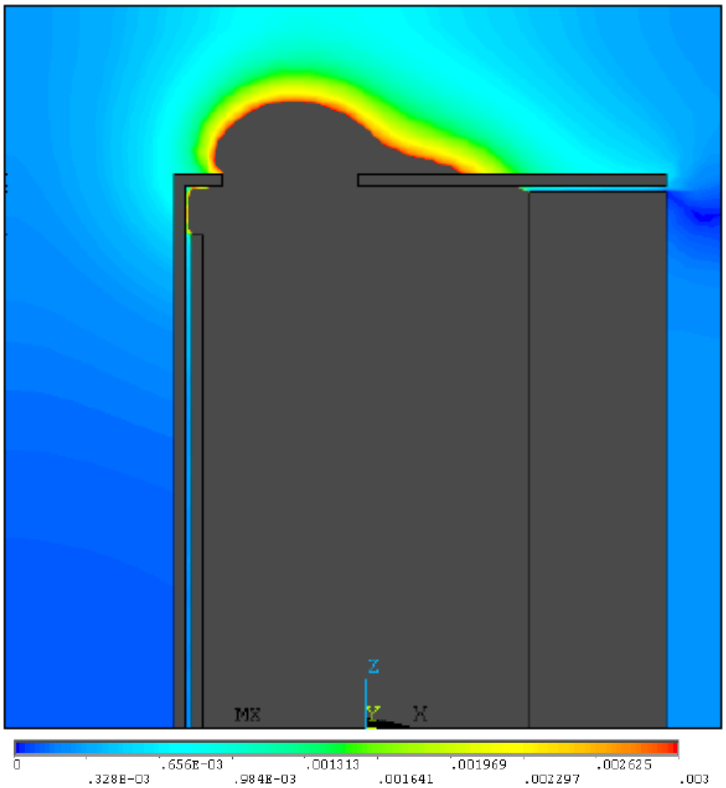

Figure 13: Magnetic flux density distribution, B_{sum}, in the orbit plane for the range $0.0<B_{sum}(T)<0.003$ after step 2.

Step 3: The thickness of the *upstream and downstream frontal screens* was increased up to a value for which the deviation angle is below the allowed limit. For this a set of screens with thicknesses increasing from 2.0 mm up to 5.0mm with the step 0.5mm was studied. As a result it was found that for the screen thickness equal to 5 mm the magnetic field integral value is 2.2321×10^{-5} Tm and the angle of deviation of the 50.5 MeV orbit is 0.1326 mrad so that the condition is fulfilled. The magnetic field distribution B_{sum} is shown in Fig.14. On can see that the introduced modification of the screen geometry has lead to a further decrease of the stray field level outside the extraction magnet (compare Fig. 14 to Fig. 11 and Fig. 13).

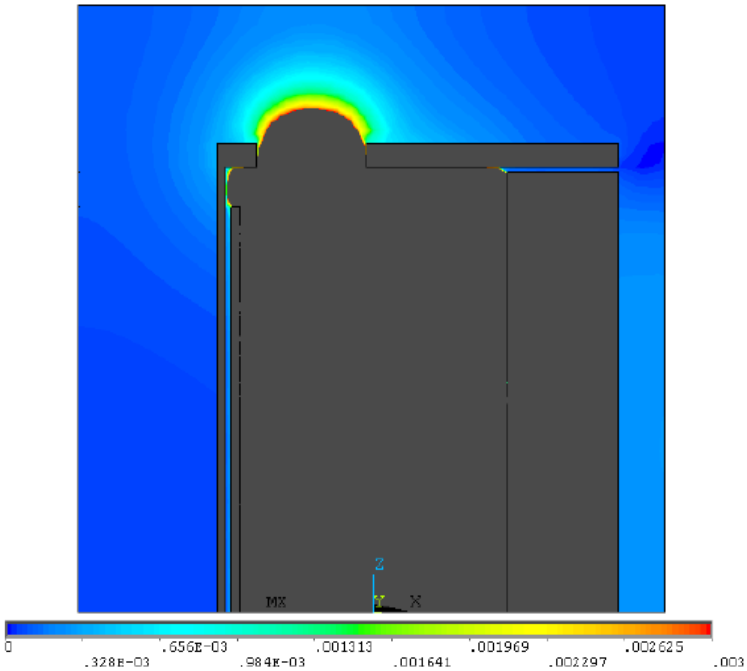

Figure 14: Magnetic flux density distribution, B_{sum}, in the orbit plane for the range $0.0 < B_{sum} < 0.003$ T after step 3.

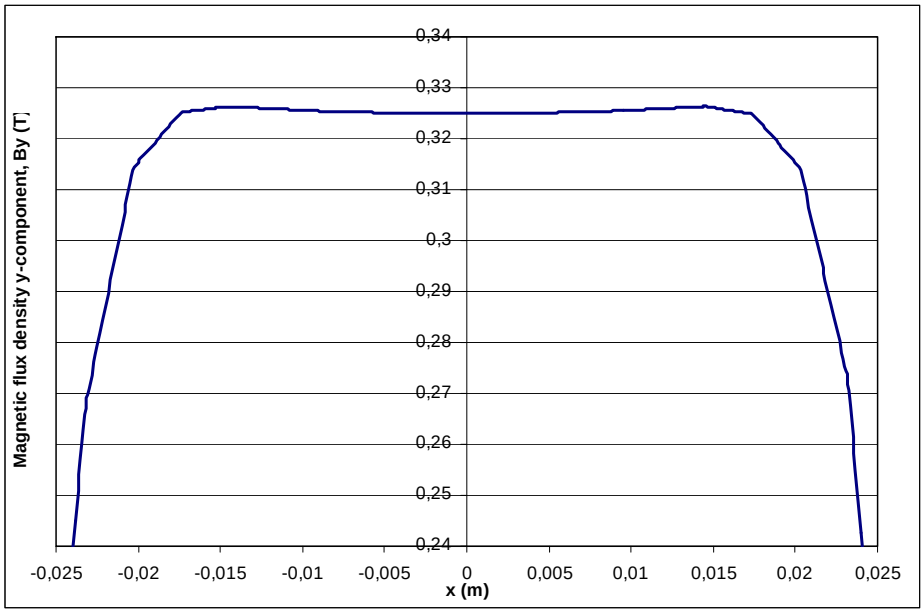

Figure 15: *y*-component of the magnetic flux density, B_y (x,0,0), in the orbit plane y=0 and in the centre of the magnet z=0.

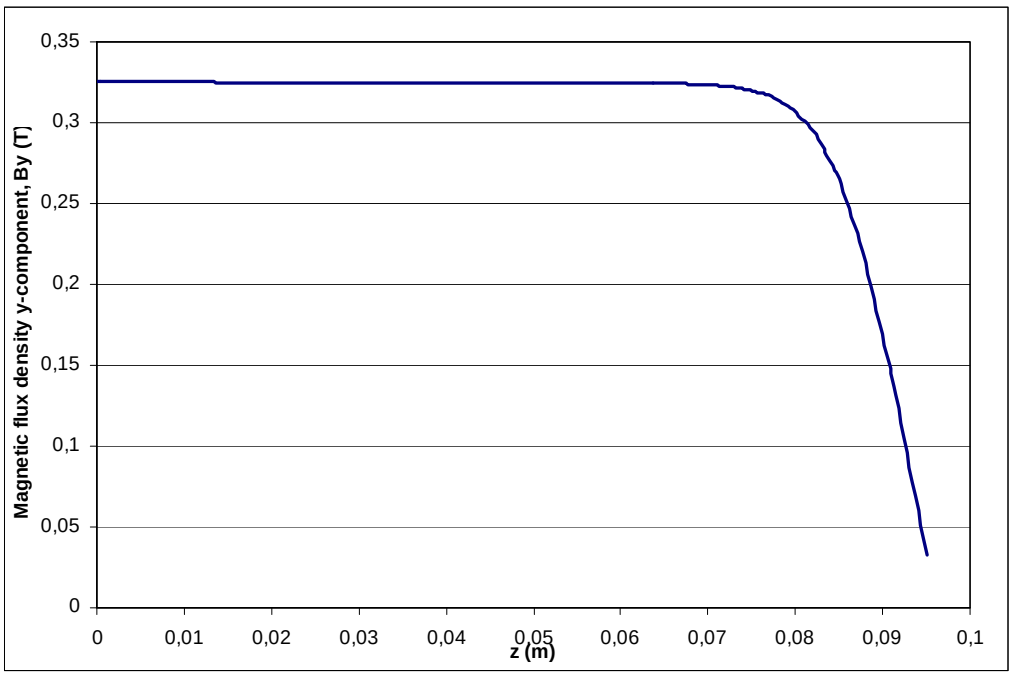

Figure 16: Magnetic flux density *y*-component, $B_y(0,0,z)$, as a function of *z*.

The transverse and longitudinal field distributions for the screen system design obtain after all three steps of optimization are given in Figs. 15 and 16. Namely, in Fig. 15 the behaviour of the y-component of the magnetic induction $B_y(x,0,0)$ at z=0, y=0 as a function of x is plotted. Magnetic field profile $B_y(0,0,z)$ in the longitudinal direction in the range $0< z < 9.5$ cm for x=0, y=0 is shown in Fig.16.

For the sake of comparison the plots of the magnetic field profiles in the longitudinal direction of the 55.5 MeV orbit for the three screen designs described above are given in Fig.17. As it can be seen, the installation of the screens leads to a reduction of the fringe field at the entrance of the extraction magnet.

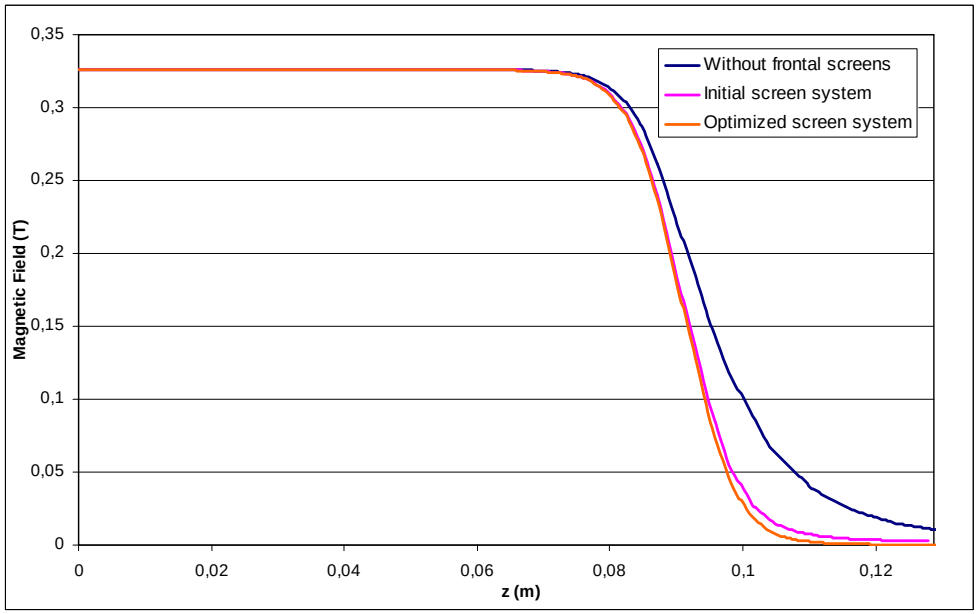

Figure 17: Magnetic field profiles for the three screen system designs.

To summarize, we propose to equip the extraction magnet of the 55.5 MeV RTM with the following screens (see Fig.18):

1. Lateral screen with the thickness 2 mm and length 200mm,
2. Upstream and downstream screens with dimensions 85x190x5 mm with a circular aperture of the radius 12 mm.

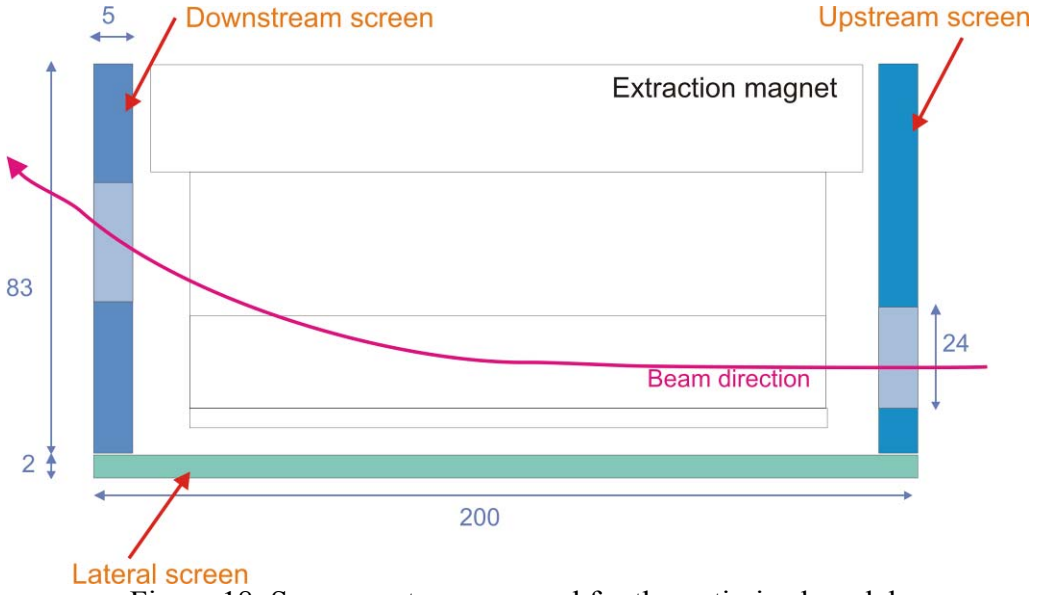

Figure 18: Screen system proposed for the optimized model.

5. - Magnetic measurements.

The optimized screen system was machined and installed at the extraction magnet (Fig. 19). The next step was to check its performance and compare results of magnetic measurements with the results of the ANSYS simulations.

(a) (b)

Figure 19: New upstream (a) and downstream (b) screens.

The magnetic test bench at which the measurements were carried out is shown in Fig.20. The extraction magnet is placed at platform (1) which is fixed on table (2). The

magnetic field induction is measured by Caylar GM-H103 Hall Gaussmeter (3) (Fig.21) with a probe fixed at copper stem (4) which can be moved in the *x*-direction along rail (5). The stem in its turn is attached to a support movable in the *z*-direction along rail (6). The Hall probe position with respect to the extraction magnet in the vertical (*y*) direction can be adjusted by displacing platform (1) with respect to table (2).

We measured the field distribution for three different versions of the extraction magnet: (1) without screens, (2) with the original screens and (3) with the optimized screens. For each of these configurations two types of measurements were carried out:

(a) Measurements of the magnetic field distribution outside the extraction magnet to determine the stray fields, with the aim to analyze their influence on the 50.5 MeV beam and verify the results obtained with the ANSYS code. In Fig.22 the region of these measurements is shown.

(b) Measurements of the magnetic field profile along the trajectory of the 55.5 MeV orbit with the aim to study the influence of the screen system on the fringe field profile and the nominal magnetic field value in the working region.

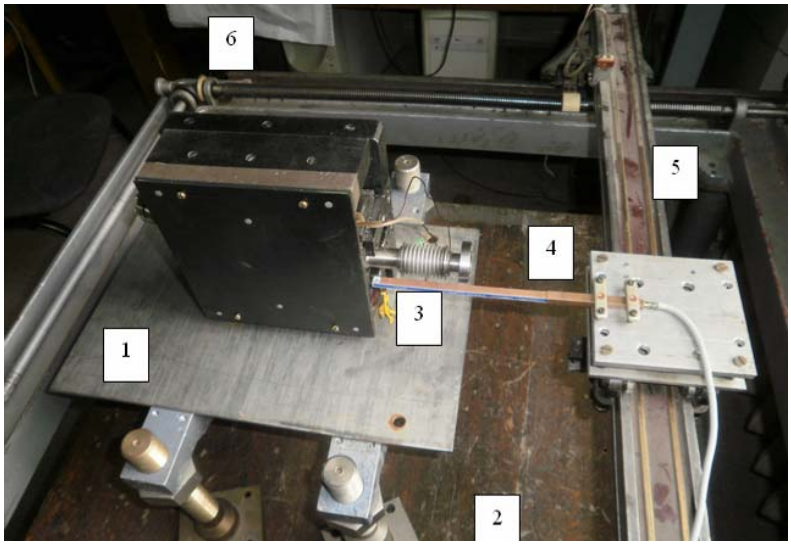

Figure 20: Magnetic test bench.

Figure 21: Caylar GM-H103 Hall Gaussmeter.

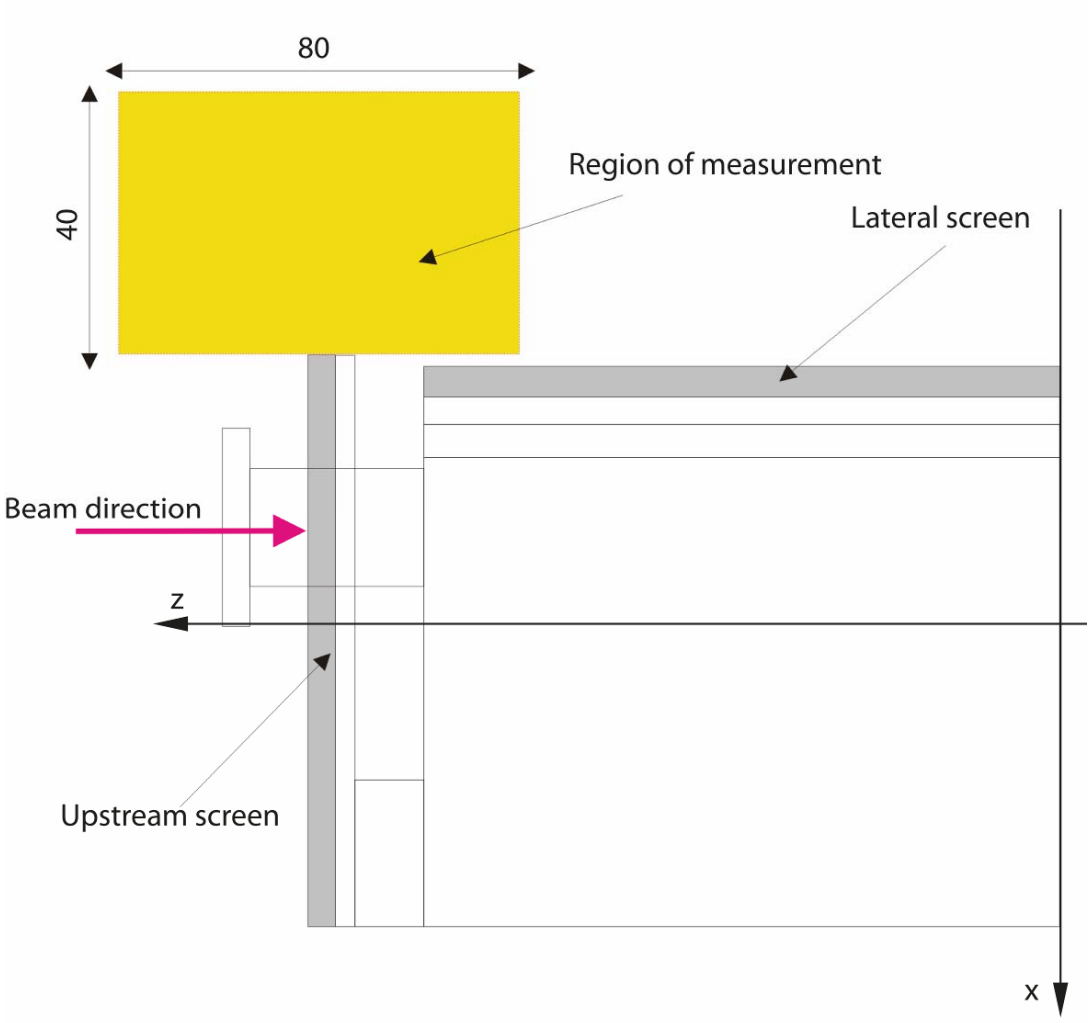

Figure 22: Region of measurement (dimensions are in mm).

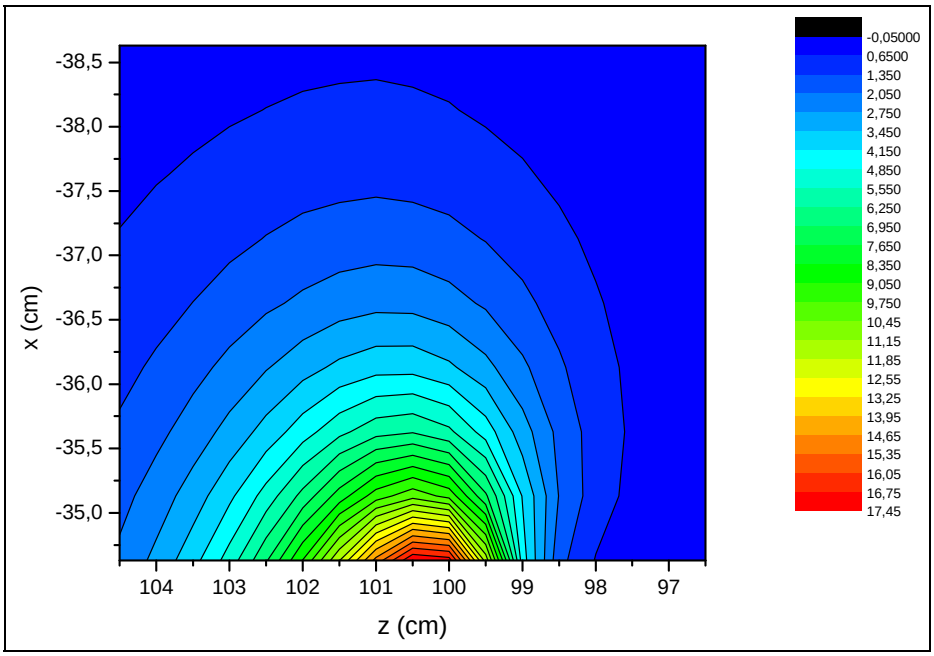

(a)

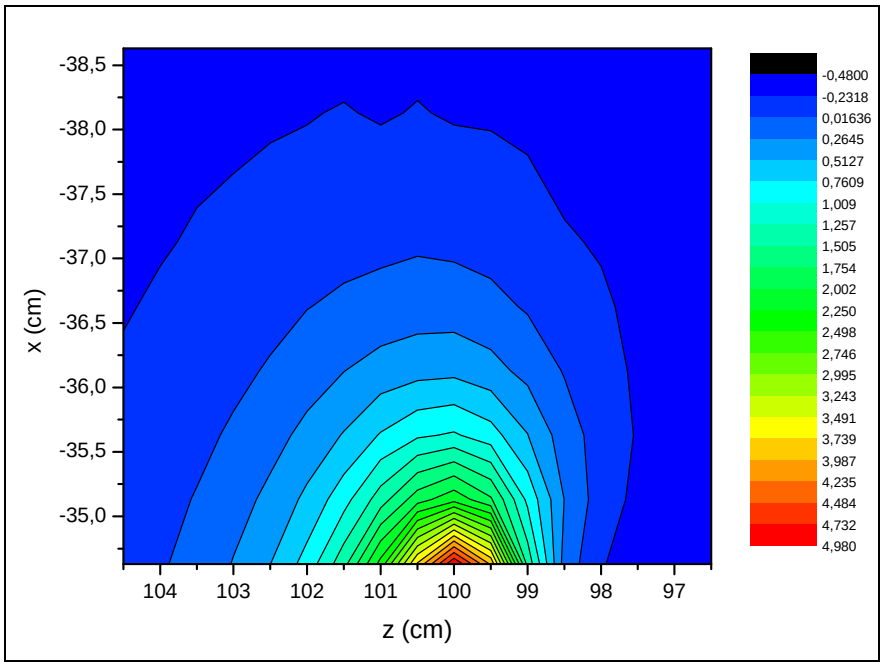

(b)

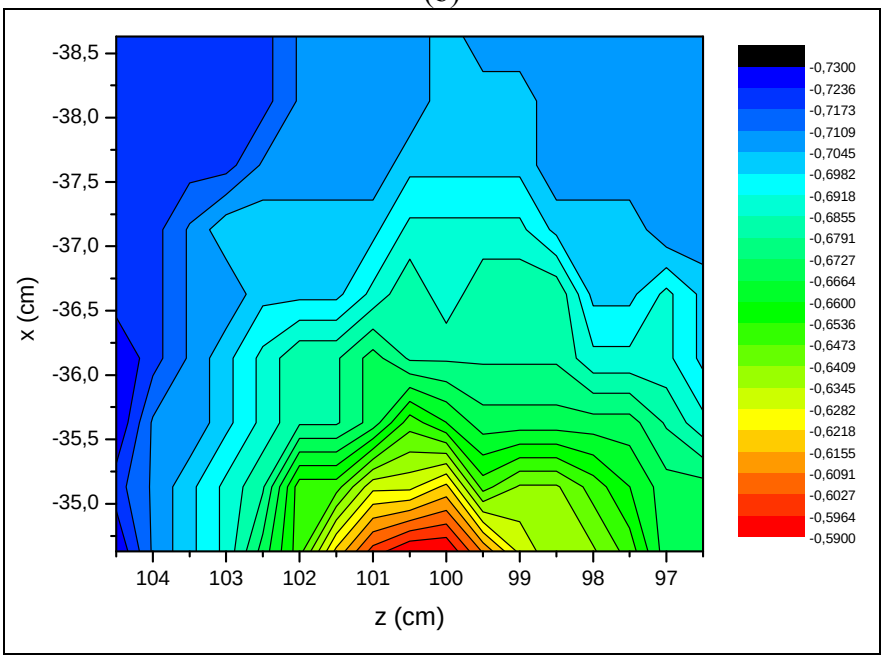

(c)

Figure 23: Magnetic field maps in the region of measurement: (a) without screens, (b) with the original screens and (c) with optimazied screen (field induction is given in mT).

The magnetic field distributions in the region of measurements for the three designs described above are given in Fig.23. One can see that in all three cases the maximum level of the stray field is reached at the end of the lateral screen (z=100 mm). Installation of the upstream screen reduced the field level in this region for about four times (Fig. 23 (b)). The increase of the upstream screen thickness in combination with closing the gap between the upstream and lateral screens reduced field to the level of a background magnetic field in the laboratory and sensitivity of magnetometer, i.e. to less than 1 G (Fig. 23 (c)). Some traces of the field near z = 100 mm in this case are explained by effects of lateral screen saturation effect.

In Fig.24 the magnetic field profiles along the 55.5 MeV orbit for the original screen system and the optimized one are shown. As one can see for the case of the original screen the magnetic field at z=0 has the required value 0.325 T. In the case of the optimized screens the magnetic field is by 0.4% lower. Thus, in order to get the required magnetic field in the working region it will be necessary to power the extraction magnet excitation coils.

In Fig. 25 and 26 a comparison of the experimental results with the ANSYS simulations for two versions of the extraction magnet, with the original screens and with the optimized screens, is given. Let us recall that in the simulations the value of the residual magnetization was set to be 0.97814 T. Inside the extraction magnet the experimental results coincide with the theoretical ones up to the end of the magnet pole at z=0.09 m (see Fig.25). The largest difference between the curves is equal to ΔB=0.021 T at z=0.1 m and is due to a difference between the real and simulated beam holes. For the case of the optimized screen system the experimental data practically coincide with the ANSYS simulations (Fig. 26).

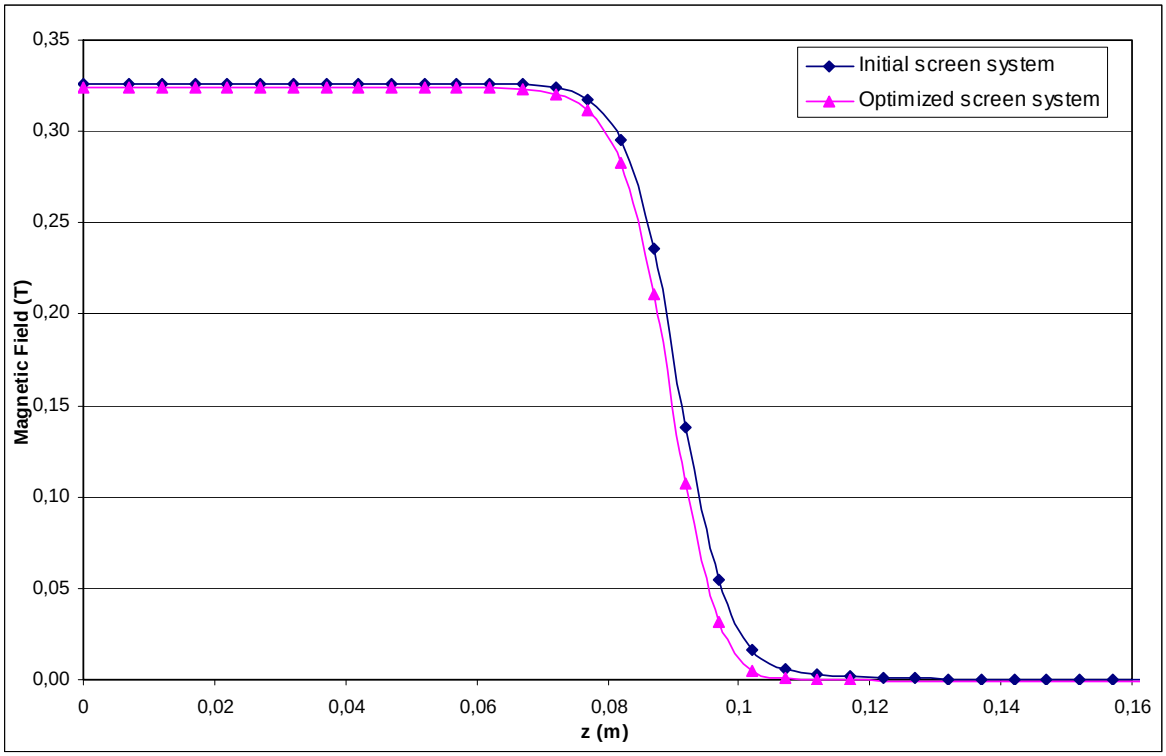

Figure 24: Magnetic field profile in the range 0<z<0.13 cm and *x*=-13.5 cm for two versions of the extraction magnet, with the original screens and with the optimized screens.

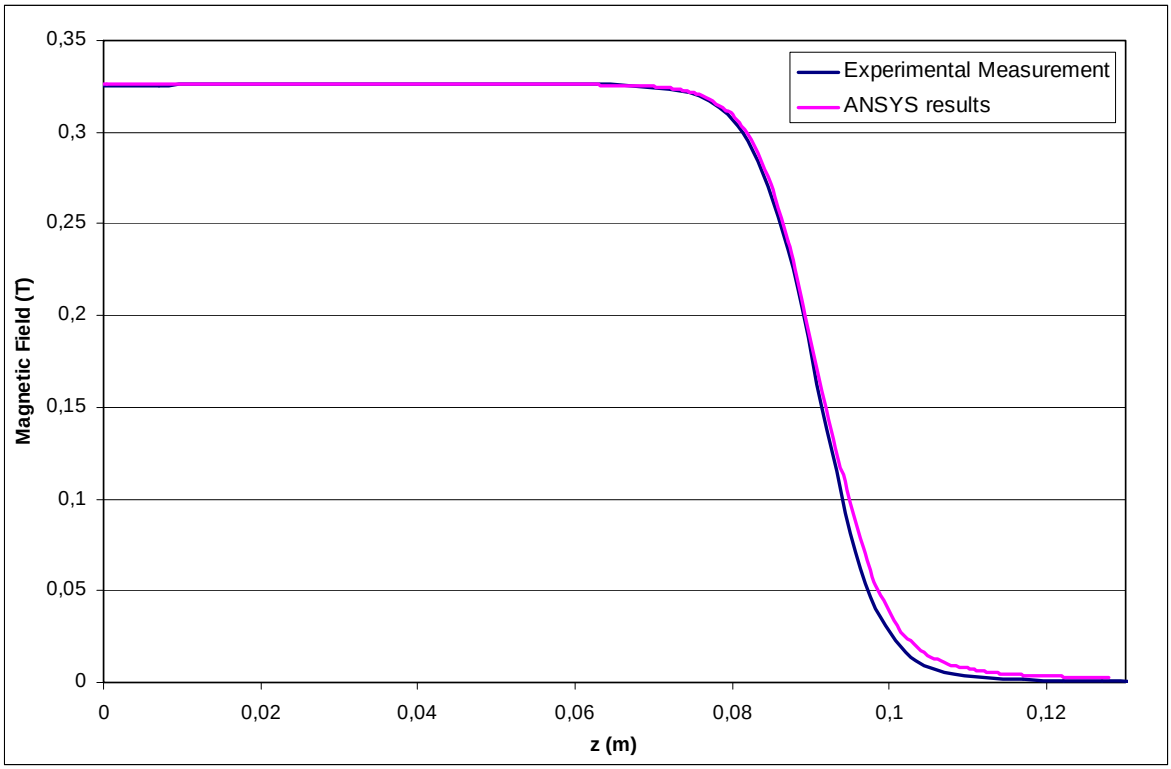

Figure 25: Magnetic field profile for the original screen system (x=-13.5 cm): Experimental measurement and ANSYS results.

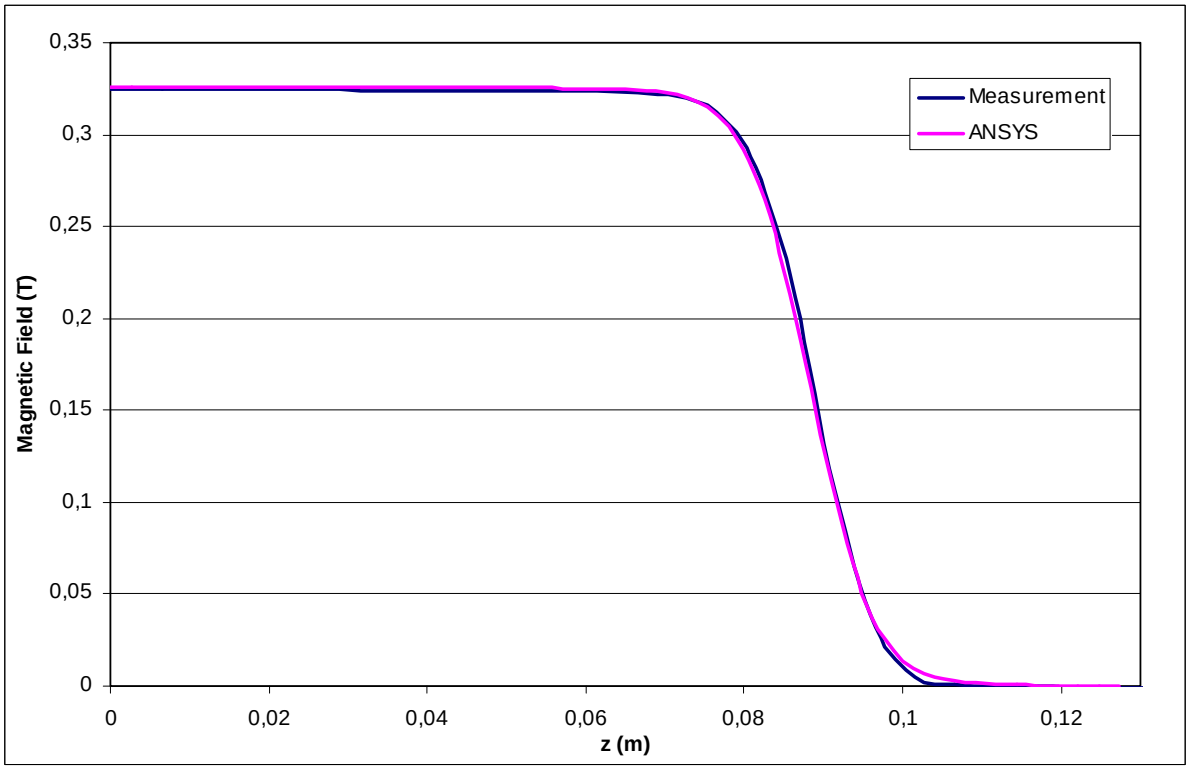

Figure 26: Magnetic field profile for the optimized screen system (x=-13.5 cm): Experimental measurement and ANSYS results.

6. – Summary and conclusions.

In this paper we described the design and discussed results of optimization of a screen system of a hybrid extraction magnet of the 55 MeV RTM. The purpose of this system is to reduce the stray magnetic fields outside the extraction magnet. The optimization was done by 3D simulations of the magnetic field with the ANSYS code.

We carried out measurements of the stray magnetic field in the region shown in Fig. 22 and compared the experimental results with the results of the ANSYS simulations. We conclude that there is a good agreement between these data.

After the installation of the screen system the magnetic stray field outside the extraction magnet has been reduced considerably (see Figs. 11, 13 and 14), so that the deviation of the neighbor orbit (50.5 MeV energy orbit) caused by this field is below the acceptable level of 15 mrad.

The new screen system reduces the magnetic field in the working region by 0.4%. Thus, in order to get the required magnetic field in this region it is necessary to use the excitation coils to adjust field level.

7. – Acknowledgements

We are grateful to B.S. Iskhanov for support of this work. The work was supported by grants VALTEC09-2-0035 of CIDEM and 2009 SGR 1516 and 2010 PAS 0030 of AGAUR (both of the Generalitat of Catalonia).

8. – References.

1.A.I. Karev, A.N. Lebedev, V.G. Raevsky, P.N. Lebedev, A.N.Kamanin, N.I. Pahomov, V.I. Shvedunov, 55 MeV Race-Track Microtron Of Lebedev Institute, XXI Russian Particle Accelerator Conference RuPAC-2008, Contributions to the Proceedings, p. 124-126
http://accelconf.web.cern.ch/AccelConf/r08/papers/TUAPH10.pdf

2. A.I.Karev, A.N.Lebedev, V.G.Raevsky, A.N.Ermakov, A.N.Kamanin, V.V.Khankin, N.I.Pahomov, V.I.Shvedunov, N.P.Sobenin, L.Brothers, L.Wilhide, 55 MeV special purpose race-track microtron commissioning, XXII Russian Particle Accelerator Conference RuPAC-2010, Contributions to the Proceedings, p. 316-318
http://accelconf.web.cern.ch/AccelConf/r10/papers/THCHD01.pdf

3. ANSYS, http://www.ansys.com

Андрей Николаевич Ермаков[1)]
Вадим Анатольевич Ханкин[1)]
Юрий Александрович Кубышин[1,2)]
Николай Иванович Пахомов[1)]
Хуан Пабло Ригла[2)]
Василий Иванович Шведунов[1)]

[1]Научно-исследовательский институт ядкрной физики МГУ, 119192, Москва, Ленинские горы 1(5)
[2]Universitat Politècnica de Catalunya Jordi Girona 31, Barcelona, Spain

РАЗРАБОТКА И МАГНИТНЫЕ ИЗМЕРЕНИЯ МАГНИТА ВЫВОДА 55 МэВ РАЗРЕЗНОГО МИКРОТРОНА

Препринт НИИЯФ МГУ –№ 2011 – 2/866

Работа поступила в ОНТИ 03.04.2011